Spatial Anisotropy of Induced Optical Effects in Crystalline Materials

Spatial Anisotropy of Induced Optical Effects in Crystalline Materials

By

A. S. Andrushchak,
O. A. Buryy,
N. A. Andrushchak
and N. M. Demyanyshyn

Cambridge
Scholars
Publishing

Spatial Anisotropy of Induced Optical Effects in Crystalline Materials

By A. S. Andrushchak, O. A. Buryy, N. A. Andrushchak
and N. M. Demyanyshyn

This book first published 2023

Cambridge Scholars Publishing

Lady Stephenson Library, Newcastle upon Tyne, NE6 2PA, UK

British Library Cataloguing in Publication Data
A catalogue record for this book is available from the British Library

ISBN (10): 1-5275-1199-5
ISBN (13): 978-1-5275-1199-6

CONTENTS

ABBREVIATIONS

AOE − acousto-optic effect
ElOC − elasto-optic coefficient
ElOE − elasto-optic effect
EOC − electro-optic coefficient
EOE − electro-optic effect
ES − extreme surface
IS − indicative surface
LN − lithium niobate, $LiNbO_3$
PEC − piezo-electric coefficient
PEE − piezo-electric effect
POC − piezo-optic coefficient
POE − piezo-optic effect

LIST OF FIGURES AND TABLES

Figures

Tables

SUMMARY

In the first volume of this monograph we address analytical description and geometric representation of the spatial anisotropy of induced optical effects in crystalline materials of different symmetry classes, as well as experimental methods and apparatus for the comprehensive study of electro-, piezo-, elasto- and acousto-optic phenomena in crystalline solids. Following experimental studies and relevant analytical calculations, we perform 3D analysis of the anisotropies of linear electro-optic, piezo-optic, elasto-optic, acoustic and acousto-optic properties of various crystalline materials and construct indicative or extreme surfaces describing the anisotropy effect.

On this basis, a consistent technology for improving the components and solid-state optoelectronics devices has been developed. In particular, it increases the efficiency of operational characteristics of the devices for controlling electromagnetic radiation, e.g. light modulators, deflectors, sensors and filters. The resources and the efficiency of this technology are demonstrated on the example of electro-, piezo-, elasto- and acousto-optic effects, although it can also be used for the other physical effects described by higher-rank tensors. The prospects of the above technology for nonlinear optics and design of novel anisotropic crystalline nano-composites are also analyzed.

The monograph would be of interest to specialists in the fields of solid-state physics, optoelectronics, acousto-electronics and optical instrumentation.

INTRODUCTION

Crystalline solids, which represent anisotropic materials, are widely used in various opto- and acousto-electronic devices. The vast majority of the crystals known up to now have a low symmetry and belong to either middle or lower crystallographic categories. According to the characteristics associated with the influences of external electric and magnetic fields, mechanical stresses, acoustic waves or laser radiation on the optical properties, low-symmetry crystals are often the most promising for applications. A prominent example is optically biaxial crystals for nonlinear-optical frequency converters. However, fundamental studies and the practical utilization of such solids are hindered by significant anisotropy of their properties. Moreover, the latter makes it difficult even to determine their basic physical and operational characteristics.

Even in the cubic crystals, of which the physical properties described by second-rank tensors are isotropic, the higher-order effects (e.g., electro-, piezo- and acousto-optic interactions) are anisotropic. As a result, the problems associated with the anisotropy are also typical for these, otherwise 'optically isotropic', crystalline materials. As a result, comprehensive study of the influence of external fields on the physical properties of crystalline solids characterized by higher-order tensors require a proper knowledge of the anisotropy of the corresponding effects.

On the other hand, this seeming drawback of anisotropic materials can readily transform into a kind of advantage. Namely, study of the anisotropy of the physical properties of low-symmetry materials by constructing the indicative surfaces of angular distributions of their response to the external fields, and a consistent analysis of these surfaces, including a search for their extreme values, yield significantly increased efficiency of these materials for controlling laser radiation. This approach can develop a scientific basis of technologies aimed at improving the performance of solid-state optoelectronic devices, including those designed to control electromagnetic radiation via electro-, piezo- and acousto-optic effects, e.g. light modulators, deflectors, sensors and filters.

It is also important that our OPTIMA technology, which has been developed in order to find the maxima of the induced optical effects, is intensive rather than extensive, since it requires neither the structural modification of already available crystalline materials nor the search for

completely new materials. It puts into effect some hidden resources, which are often inherent even in canonical and widely known materials, due to their anisotropy and the availability of 'hidden' optimal directions of propagation and polarization of light, as well as optimal directions of external fields, for which the quantitative characteristics of a crystal reach their maxima. This follows from our fundamental conclusion: the global maxima of externally induced optical effects for most anisotropic materials often do not coincide with the principal axes of crystallographic coordinate system and, sometimes, these maxima do not even lie in the principal planes of this coordinate system. In other words, many practical situations indicate that the techniques like our OPTIMA technology are indeed in demand.

The present monograph describes the main ideas and approaches underlying the OPTIMA technology for investigating the anisotropy of externally induced optical effects in crystalline materials. The first volume of the monograph is devoted mainly to theoretical issues, in particular the analytical description and geometric representation of the anisotropy of optical or acoustic effects, and experimental techniques which have been adopted and improved by the authors for studying anisotropic crystalline materials.

The second volume will deal with the typical results of 3D analysis of the spatial anisotropy of electro-, piezo-, elasto- and acousto-optic effects. They will refer to both commonly known model materials ($LiNbO_3$, SiO_2, etc.) and new promising crystals, which have been studied by the authors.

Up to now, the relevant results have been scattered over many scientific and technical periodicals, and conference materials. This monograph represents our attempt to systematize and generalize the corresponding data and conclusions.

CHAPTER 1

ANALYTICAL DESCRIPTION OF ELECTRO-OPTIC AND PHOTO-ELASTIC PHENOMENA IN ANISOTROPIC MATERIALS

1.1. Linear electro-optic effect

1.1.1. Brief review

Linear electro-optic effect (EOE) has already found wide practical applications in various solid-state electronics devices [1, 2]. The interest in its study remains high enough [3−5], especially in relation to the rapid development of novel technologies and the appearance of new promising crystalline materials [6−8]. High-performance electro-optic crystals often belong to low-symmetry classes and reveal significant anisotropy. In order to use these crystals as working elements of various optoelectronic devices in an optimal manner, one has to study analytically the manifestations of EOE in different experiments and analyze the spatial (angular) distribution of the effect. This can be implemented after determining experimentally all nonzero components of the electro-optic tensor (i.e., electro-optic coefficients abbreviated hereafter to EOCs) and constructing, on this basis, so-called indicative surfaces (ISs) or extreme surfaces (ESs), as explained in Chapter 2. A ready example of this approach has been demonstrated for the cases of piezo-optic effect (POE) and elasto-optic effect (ElOE) in References [9−11].

Of course, the measurements of EOCs for the crystals of different (most often, high) symmetry classes have been performed in many laboratories worldwide (see, e.g., works [12, 13] and references therein). However, the literature has not described a general enough technique which would enable determining all the absolute EOCs for the crystals of arbitrary symmetry classes. So, the formulae that describe the changes in the principal refractive indices under the influence of the electric field have been obtained in works [12, 14]. Nonetheless, they do not consider the most general case of triclinic crystals. Moreover, these formulae

cannot be used in practice for the experimental determination of non-principal EOCs, because they do not take the piezo-electric deformation of sample into account, which can become a source of gross experimental errors. In addition, study [14] does not consider the phenomenon of 'sign dualism' for a number of non-principal EOCs. Furthermore, the formulae available in Reference [14] for most of the rotary EOCs imply that the latter coefficients can only be determined following the field-induced rotations of optical indicatrix. For many practical reasons, this method cannot be implemented experimentally. (Note that Subsection 1.1.3 introduces the formulae for determining the rotary EOCs, which are based directly on the field-induced refractive-index changes.)

In this chapter, we provide a general theoretical analysis of the experimental manifestations of the linear EOE in the crystals of arbitrary symmetries, with the emphasis on interferometric measurements. It is these experiments that provide the most accurate information about the EOCs. They have enabled us to solve a problem that most researchers do not even pay much attention to. This problem is separating reliably the contributions of EOE and piezo-electric effect (PEE) into the electric field-induced changes of optical path difference, i.e. separating the corresponding changes in the refractive indices and the changes in the thickness of crystal (see References [14, 15]). Subsection 1.1 describes also an interferometric technique employed in so-called twofold EOC measurements, which result in higher accuracy of all the absolute EOCs for the crystals of arbitrary symmetry classes [16−20].

1.1.2. General description of electro-optic phenomena in crystals

Linear EOE, termed also the Pockels effect, is described by a linear change in refractive indices induced by an external electric field [14, 21]. Since the propagation of electromagnetic waves in crystals without considering spatial dispersion (see works [22, 23]) is completely described by the ellipsoid of refractive indices, the influence of the electric field can be thought of as a change in the optical indicatrix. Its equation,

$$a_{ij}x_i x_j = 1\,, \tag{1.1}$$

defines a triaxial ellipsoid, with a_{ij} being the components of dielectric impermeability tensor (or a so-called tensor of optical polarization constants) and x_i, $x_j = x_1, x_2, x_3$ denoting the coordinates which are mainly associated with the principal coordinate system (termed a 'crystal–physical' system hereafter).

When a low-frequency electric field $\boldsymbol{E} = (E_x, E_y, E_z)$ is applied to a crystal, its optical polarization constants a_{ij} change (see References [12, 14]) according to the relation

$$\Delta a_{ij} = r_{ijk} E_k + R_{ijkl} E_k E_l + \dots . \tag{1.2}$$

Here r_{ijk} imply the components of a polar third-rank tensor symmetric in its first two indices, which describes the linear EOE, and R_{ijkl} are the components of a polar fourth-rank tensor symmetric in its first two and last two indices, which describes a quadratic EOE (or a Kerr effect).

Consider the linear EOE and the symmetry of the EOCs r_{ijk}. We introduce well-known (see, e.g., References [24, 25]) matrix notations 11→1, 22→2, 33→3, 23 (32)→4, 13 (31)→5 and 12 (21)→6. When neglecting the terms of higher E_i powers in formula (1.2), one can obtain the relation

$$\begin{pmatrix} \Delta a_1 \\ \Delta a_2 \\ \Delta a_3 \\ \Delta a_4 \\ \Delta a_5 \\ \Delta a_6 \end{pmatrix} = \begin{pmatrix} r_{11} & r_{12} & r_{13} \\ r_{21} & r_{22} & r_{23} \\ r_{31} & r_{32} & r_{33} \\ r_{41} & r_{42} & r_{43} \\ r_{51} & r_{52} & r_{53} \\ r_{61} & r_{62} & r_{63} \end{pmatrix} \begin{pmatrix} E_1 \\ E_2 \\ E_3 \end{pmatrix}. \tag{1.3}$$

As follows from symmetry consideration, we have $r_{mk} = 0$ for the crystals with inversion centre [14, 26]. The form of the EOC matrix r_{mk} for the other (non-centrosymmetric) crystals can be found from the analysis of point symmetry, which also allows for clarifying relationships among particular coefficients [25].

Consider as an example a description of EOE in lithium niobate, $LiNbO_3$, which is abbreviated to LN [13]. This crystal is optically uniaxial. It is described by point group 3*m*, for which the linear EOE is allowed by symmetry. The EOC matrix for the crystals of this point group has the following form [25]:

$$\left(r_{\mu k}\right) = \begin{pmatrix} 0 & -r_{22} & r_{13} \\ 0 & r_{22} & r_{13} \\ 0 & 0 & r_{33} \\ 0 & r_{51} & 0 \\ r_{51} & 0 & 0 \\ -r_{22} & 0 & 0 \end{pmatrix}. \tag{1.4}$$

When the electric-field component E_y is applied, the LN crystal becomes optically biaxial. Then there appears an induced birefringence along the *Z* direction [14]:

$$\delta(\Delta n) = n_o^3 r_{22} E_y, \tag{1.5}$$

where n_o is the ordinary refractive index.

Since a general relation $\delta a_i = \delta\left(\frac{1}{n_i^2}\right) = -\frac{2\delta n_i}{n_i^3}$ holds true, one can arrive at the equality $\delta(\Delta n) = \delta n_i - \delta n_j = \frac{1}{2}\left(n_i^3 \delta a_i - n_j^3 \delta a_j\right)$. If the field acts along the *Z* axis in the LN crystals and the light propagates perpendicular to this axis (e.g., along the *X* direction), then there are induced changes in the birefringence $\delta(\Delta n)$ and an optical phase difference $\delta\varphi = \frac{2\pi}{\lambda} t_x \delta(\Delta n)$. They can be calculated using a classical tensor approach [14]:

$$\delta(\Delta n) = \frac{1}{2}\left(n_o^3 r_{13} - n_e^3 r_{33}\right) E_z,$$

$$\delta\varphi = \frac{\pi t_x}{\lambda t_z}\left(n_o^3 r_{13} - n_e^3 r_{33}\right) U_z. \tag{1.6}$$

Here n_o and n_e imply respectively the ordinary and extraordinary refractive indices, λ the wavelength of light, t_x the thickness of the crystal along the direction of the light transmission, t_z the crystal length along direction *Z* of the electric field, and U_z the electric voltage applied to the crystal along this direction. Here the field-induced birefringence is a correction to the natural one, $\Delta n_0 = n_e - n_o$.

Consider another example. Let the electric field be applied along the *Z* axis in the crystals of symmetry group $\bar{4}2m$. Let the light polarized along the *X* (or *Y*) axis propagate along the *Z* axis. After passing the crystal, it acquires the phase difference $\delta\varphi$ [14, 27]:

$$\delta\varphi = \frac{2\pi}{\lambda} t\delta(\Delta n) = \frac{2\pi}{\lambda} t n_o^3 r_{63} E_z, \tag{1.7}$$

where *t* is the thickness of the crystal sample. The optical transmission *J* of a polarizer–crystal–analyzer system, in which the polarizer and the analyzer are crossed while the crystal is oriented ‘diagonally’ (i.e., the directions of its indicatrix axes under the field make the angle 45° with respect to the transmission axes of the polarizers) is determined by a known relation (see, e.g., Reference [15])

$$J = \frac{I}{I_0} = \sin^2 \frac{\delta\varphi}{2}, \tag{1.8}$$

with I and I_0 being respectively the emergent and incident light intensities. Following formulae (1.7) and (1.8), one can obtain the relationship

$$J = \sin^2 \frac{\pi}{\lambda} n_0^3 U_z r_{63} \tag{1.9}$$

for the parallel orientations of the light and the electric field.

The electric voltage $U_z = E_z d$ required to increase the optical transmission of the polarization system from zero (in the absence of a field) to unity (under the field applied) is called a half-wave voltage ($U_{\lambda/2} = \lambda/(2n_0^3 r_{63})$). It follows from formula (1.9) that this voltage does not depend on the crystal size. One of the methods for determining the EOCs of crystals just relies on the measurement of the half-wave electric voltage.

For the LN crystals (symmetry group $3m$), the half-wave voltage for the above case is given by

$$U_{\lambda/2} = \lambda d_x / 2n_o^3 r_{22} d_z . \tag{1.10}$$

It is seen from formula (1.10) that, unlike the crystals of group $\bar{4}2m$, the half-wave voltage now depends on the geometric dimensions of the sample.

Another method for studying EOE is based on the measurements of optical birefringence induced by the external electric field [28]. This is a Senarmont method, which uses a polarizer–crystal–compensator–analyzer polarization system in which the compensator is a quarter-wave phase plate. In this scheme, the polarizer and the analyzer are crossed, the major axes of optical indicatrix of the quarter-wave plate are set to be parallel to the transmission axes of polarizers, and the crystal is in 'diagonal' orientation in the presence of the field. After turning off the voltage applied to the crystal and rotating the analyzer until a minimal light intensity is achieved at the output of the polarization system, a researcher has to detect the appropriate reading α_0 of the angle-measuring mechanism of the analyzer. Then the voltage is switched on and one reads again the analyzer angle α, which corresponds to the minimum intensity in the presence of the field. Then the field-induced birefringence can be determined as [14, 15]

$$\Delta n = \frac{\lambda(\alpha - \alpha_0)}{\pi t}, \tag{1.11}$$

where t is the thickness of the crystal along the direction of the light propagation.

Sometimes, the ‘relative’ methods for determining the EOCs described above do not account for the contribution of the inverse PEE into the changes of optical path of a light beam. In other words, they are based, intentionally or not, on the approximation of invariable crystal thickness. In addition to the relative methods, one can also employ ‘absolute’ methods which are based on interferometry (see Section 3.3). The latter methods consider possible contributions of the inverse PEE into resulting electro-optic data.

Obtaining the analytical relations that describe interaction of light with a crystal under the action of the electric field in the framework of these methods is a separate complex problem. Its solutions will be obtained and discussed in the next subsection.

1.1.3. Analytical relations for the interferometric methods of determining electro-optic coefficients

We illustrate how to derive analytical relations for determining EOCs on the example of a known interferometric method [12], which is implemented, e.g., using a Mach−Zehnder interferometer. A sample under test is placed into one of the arms of this interferometer. The optical path introduced by the sample is equal to $\Delta_{ik} = (n_i - n_p)t_k$, where n_i and n_p are the refractive indices of sample and environment, respectively (e.g., the equality $n_p = 1$ is taken for the air), and t_k is the crystal size along direction $\vec{k}$ of light propagation.

Let the electric field E_l be applied to the crystal. Here $\vec{l}$ implies the direction of the electric field, whereas $\vec{i}$ defines the direction of the oscillations of the light wave, i.e. its polarization. The induced change in optical path Δ_{ikl} for the light beam passing through the sample is given by the following formula:

$$\delta\Delta_{ikl} = \delta[(n_i - 1)t_k] = t_k\delta n_i + (n_i - 1)\delta t_k = -\frac{r_{il}n_i^3}{2}E_l t_k + (n_i - 1)d_{lk}E_l t_k \,. \quad (1.12)$$

Here the first term in the r. h. s. of formula (1.12) represents the change in the optical path due to the EOE, i.e. due to changing refractive index δn_i (or a corresponding change in polarization constant δa_i) acquired under the electric field ($\delta n_i = -\frac{\delta a_i}{2a_i^{3/2}} = -\frac{r_{il}E_l n_i^3}{2}$). The second term describes the inverse PEE, i.e. a change in the optical path appearing due to changing the sample size t_k along the light propagation direction under the electric field E_l applied ($\delta t_k = d_{lk}\, E_l t_k$). Besides, r_{il} are the linear EOCs and d_{lk}

denote the PECs. Directions $\vec{i}$, $\vec{k}$ and $\vec{l}$ in a practical experiment are mainly mutually orthogonal. Nevertheless, directions $\vec{k}$ and $\vec{l}$ can coincide with each other in the case of so-called longitudinal EOE.

Electrically induced changes in the optical path would shift the interference pattern. For practical reasons, it is convenient to achieve the shift of this pattern equal to $\delta\Delta_{ikl} = n\lambda/2$ (with n = 1, 2, …) by changing continuously the electrical voltage applied to the sample. If n = 1, we have the above-mentioned 'half-wave voltage' $U_{\lambda/2}$, at which the interference minimum turns into the maximum or vice versa, which is easily detected in practice.

To determine unambiguously the signs and the absolute values of the EOCs in low-symmetric crystals, the following arguments must be taken into account.

1. The sign of the induced change in optical path $\delta\Delta_{ikl}$ under the action of positive electric field $+E_l$ must be determined by the following criterion: if the increase in E_l leads to increasing optical path, then $\delta\Delta_{ikl}$ is positive.

2. It is necessary to define the positive directions of axes of the crystal–physical coordinate system in accordance with the known rules approved by the IRE standard [29]. The latter has been supplemented by the case of POE in Reference [30].

3. It is necessary to set unambiguously the sign of the electric field. Namely, the positive direction of the electric field vector must be chosen as a direction generally accepted in physics, i.e. from positively to negatively charged poles of a power supply. Then the direction of the field in any experimental measurements must coincide with the positive direction of one of the axes of the crystal–physical coordinate system.

We emphasize that the crystallographic and crystal–physical coordinate axes of different effects often do not coincide with each other in low-symmetric crystals. Therefore, it is necessary to find out in which coordinate system the PEC components d_{lk} have been determined. Moreover, if it is necessary, one has to convert these components to the crystal–physical system, of which axes represent the principal axes of the optical-indicatrix ellipsoid.

To determine all the components of the EOC tensor for the crystals of the lowest symmetry, one needs to prepare four different samples. One sample of a direct cut (see Figure 1.1, sample #1) is needed for determining the principal coefficients (i, k, l = 1, 2, 3). Furthermore, three samples of 45°-cuts are needed in order to determine the remaining coefficients corresponding to i, k, l = 4, 5, 6. Concerning each of the principal crystal–physical axes, we refer the reader to samples ##2, 3 and 4 in Figure 1.1.

Let us show how to specify required experimental geometries so that one can determine all the components of the EOC tensor for the triclinic crystals. A standard routine here is that, in each subsequent experiment, only one 'new' (i.e., still unknown experimentally) EOC is actual. Moreover, this EOC can, in principle, involve a linear combination of some 'old' r_{il} coefficients, which have already been determined in the previous experiments. In this manner, one can derive progressively the whole EOC matrix in a number of consecutive electro-optic experiments.

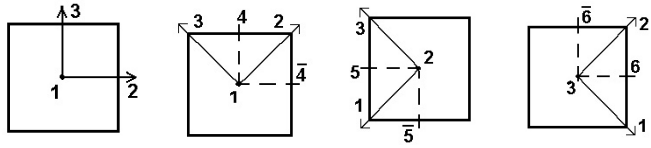

Figure 1.1. Orientations of samples needed for completing EOC matrix in the case of triclinic crystals [17]

1. In order to determine the nine independent principal EOCs (those with indices i, k, l = 1, 2, 3), so-called 'direct cuts' of crystals are used, with their faces being perpendicular to the crystal–physical axes X_1, X_2 and X_3. To determine all these coefficients, one has to direct the field along all three principal directions, one after another. Therefore, it is necessary to make three such samples with the electrodes attached to the faces (X_2X_3), (X_1X_3) and (X_1X_2). Then each of the principal EOC is calculated based on formula (1.12):

$$r_{il} = -2n_i^{-3}\frac{\delta\Delta_{ikl}}{E_l t_k} + 2n_i^{-3} d_{lk}(n_i - 1). \qquad (1.13)$$

Each of these three samples can provide three principal EOCs, for which the directions of the electric voltage E_l coincide.

Note that, when determining the principal EOCs for some optically uniaxial crystals (e.g., for those of symmetry classes 62m, 6, 32 and 3), formula (1.13) must be used for the case of r_{11} coefficient. The same is valid for the coefficient r_{22} measured for symmetry classes 6, 3m and 3. Indeed, there is no component of the inverse PEE involved in optical path change $\delta\Delta_{ikl}$ for the experimental geometries that correspond to the first (i = 1, k = 3 and l = 1) and second (i = 2, k = 3 and l = 2) cases. This is because the corresponding d_{lk} coefficients are zero in these crystals. Then the relation (1.13) becomes simplified:

$$r_{11} = -2n_1^{-3}\frac{\delta\Delta_{131}}{E_1 t_3},\quad r_{22} = -2n_2^{-3}\frac{\delta\Delta_{232}}{E_2 t_3}. \qquad (1.14)$$

2. In order to determine the rest of the EOCs (samples ##2, 3 and 4 – see Figure 1.1), so-called '45º-cut' samples are used. In general, the coefficients r_{41}, r_{52} and r_{63} can be determined on the samples for which the electrodes are attached to the faces perpendicular to directions X_1, X_2 and X_3.

The most difficult step in solving the problem of completing the EOC matrices is to derive the formulae that relate the EOCs to the induced changes in the optical path for each of the particular geometries of the interferometric experiments. A well-known approach, which consists of the analysis of the equation for the optical indicatrix perturbed by electric field [14], turns out to be cumbersome in too many cases. For the purpose of analytical description of the most complex experimental geometries of electro-optics, we use a tensor method instead (see also the corresponding analysis in Reference [33]).

The essence of the tensor method is as follows. When obtaining formulae for the EOCs, we use formula (1.12) generalized for an arbitrary ('new') coordinate system:

$$\delta\Delta'_{ikl} = -\frac{r'_{il}n'^3_i}{2}E_l t_k + d'_{lk}(n'_i - 1)E_l t_k. \qquad (1.15)$$

Here the effective values r'_{il} and d'_{il} of the tensor components are determined by the standard expressions for transforming third-rank tensors [24, 25]:

$$r'_{il} = r'_{iil} = \alpha_{if}\alpha_{ig}\alpha_{lq}r_{fgq},$$
$$d'_{lk} = d'_{lkk} = \alpha_{lq}\alpha_{kg}\alpha_{kf}d_{qgf}. \qquad (1.16)$$

In (1.16), r_{fgq} and d_{qgf} denote the components of EOE and PEE tensors in the principal coordinate system, and refractive index n'_i is linked with the optical polarization constants a_{ii} by a known expression,

$$n'_i = 1/\sqrt{a'_i} = 1/\sqrt{\alpha_{ig}^2 a_{gg}} = 1/\sqrt{\alpha_{ig}^2 n_g^{-2}}. \qquad (1.17)$$

Here $\alpha_{lq}, ..., \alpha_{kf}, ..., \alpha_{ig}, ...$ are the direction cosines of the axes of an 'old' (i.e., crystal–physical) coordinate system with respect to the directions of field (*l*), light propagation (*k*) and light polarization (*i*).

To determine the coefficient r_{41}, one should use sample #2 (see Figure 1.1) with electrodes attached to the face perpendicular to the X_1 direction. Then the two experimental geometries can possibly be used for determining r_{41}: $i = 4$, $k = \bar{4}$ and $l = 1$ (we call them 'direct conditions')

and $i = \bar{4}$, $k = 4$ and $l = 1$ (we call them 'symmetric conditions' of the above direct conditions). Here '4' denotes a diagonal of the positive directions of the X_2 and X_3 axes, and direction $\bar{4}$ is perpendicular to axis 4. Note that simultaneous utilization of these direct and symmetrical conditions represents a basis of a so-called twofold method of EOC measurements (see References [17, 18]).

It is interesting that the signs of the r_{41} and d_{14} terms in the formulae given below would depend on the choice of signs of the crystal–physical coordinate axes [29, 30]. For the above experimental conditions, the direction cosines for the light polarization are given by $\alpha_{i1} = 0$, $\alpha_{i2} = \sqrt{2}/2$ and $\alpha_{i3} = \pm\sqrt{2}/2$ (hereinafter the lower signs '+' or '–' refer to the symmetrical conditions of the experiment). For direction $\vec{k}$ of the light propagation, we have $\alpha_{k1} = 0$, $\alpha_{k2} = \sqrt{2}/2$ and $\alpha_{k3} = \mp\sqrt{2}/2$, while the relations $\alpha_{l1} = 1$, $\alpha_{l1} = 0$ and $\alpha_{l1} = 0$ hold true for direction $\vec{l}$ of the electric field. Substituting these direction cosines into formulae (1.16) and (1.17), we arrive at the expressions for the effective r'_{il}, d'_{kl} and n_i parameters:

$$r'_{41} = \frac{1}{2}\left(r_{21} + r_{31} \pm 2r_{41}\right),\ d'_{14} = \frac{1}{2}\left(d_{12} + d_{13} \mp d_{14}\right),$$
$$n_4 = \sqrt{2}\Big/\sqrt{n_2^{-2} + n_3^{-2}}\ . \tag{1.18}$$

After substituting formula (1.18) into (1.15) and solving it with respect to r_{41}, we obtain the expressions for the EOC r_{41}, which are valid for the crystals of the lowest symmetry under direct and symmetric conditions. These formulae are given in the first two rows of Table 1.1.

After combining the latter formulae, one obtains a significantly simpler formula (T.1) (see Table 1.2) for determining the EOC r_{41}. This formula does not involve the EOCs r_{21} and r_{31}, as well as the PECs d_{12} and d_{13}. This makes it possible to obtain a more accurate r_{41} value, by analogy with the method suggested in our work [11] for the POE. Therefore, the method of twofold measurements increases the accuracy of interferometric methods for determining the EOCs.

Table 1.1 shows the expressions derived for the components r_{41}, r_{52} and r_{63}, as well as the corresponding errors of their determination. The latter are calculated as a standard deviation of the mean errors for all the measurables $\delta\Delta_{ikm}$, E_l and d_{lk}, which are included in the operating relations. The errors of the latter parameters have been taken to be equal to 3%, 2% and 3%, respectively. From the formulae of Table 1.1, one can obtain the relations for the EOCs r_{41}, r_{52} and r_{63} (the corresponding relations are

presented in Table 1.2), as well as some convenient relations used within the method of twofold measurements for the other EOCs.

Table 1.1. Basic relations for determining non-principal EOCs r_{il} in the crystals of triclinic symmetry [17]

Sample (see Figure 1.1)	Working relation	Calculated error
#2	$r_{41} = -2n_4^{-3}\dfrac{\delta\Delta_{4\bar{4}1}}{t_{\bar{4}}E_1} + n_4^{-3}(n_4-1)$ $\times(d_{12}+d_{13}-d_{14})-(r_{21}+r_{31})/2$	9%
	$r_{41} = 2n_4^{-3}\dfrac{\delta\Delta_{\bar{4}41}}{t_4E_1} - n_4^{-3}(n_4-1)$ $\times(d_{12}+d_{13}+d_{14})+(r_{21}+r_{31})/2$	9%
#3	$r_{52} = 2n_5^{-3}\dfrac{\delta\Delta_{5\bar{5}2}}{t_{\bar{5}}E_2} + n_5^{-3}(n_5-1)$ $\times(d_{21}+d_{23}-d_{25})-(r_{12}+r_{32})/2$	9%
	$r_{52} = 2n_5^{-3}\dfrac{\delta\Delta_{\bar{5}52}}{t_5E_2} - n_5^{-3}(n_5-1)$ $\times(d_{21}+d_{23}+d_{25})+(r_{12}+r_{32})/2$	9%
#4	$r_{63} = -2n_6^{-3}\dfrac{\delta\Delta_{6\bar{6}3}}{t_{\bar{6}}E_3} + n_6^{-3}(n_6-1)$ $\times(d_{31}+d_{32}-d_{36})-(r_{13}+r_{23})/2$	9%
	$r_{63} = 2n_6^{-3}\dfrac{\delta\Delta_{\bar{6}63}}{t_6E_3} - n_6^{-3}(n_6-1)$ $\times(d_{31}+d_{32}+d_{36})+(r_{13}+r_{23})/2$	9%

Table 1.2. Relations for determining non-principal EOCs for the crystals of triclinic symmetry with the method of twofold measurements [17]

Sample (see Figure 1.1)	Working relation	Formula	Calculated error
#2	$r_{41} = -n_4^{-3}\left(\frac{\delta\Delta_{4\bar{4}1}}{t_{\bar{4}}E_1} - \frac{\delta\Delta_{\bar{4}41}}{t_4E_1}\right) - n_4^{-3}(n_4-1)d_{14}$	(T.1)	6%
#3	$r_{52} = -n_5^{-3}\left(\frac{\delta\Delta_{5\bar{5}2}}{t_{\bar{5}}E_2} - \frac{\delta\Delta_{\bar{5}52}}{t_5E_2}\right) - n_5^{-3}(n_5-1)d_{25}$	(T.2)	6%
#4	$r_{63} = -n_6^{-3}\left(\frac{\delta\Delta_{6\bar{6}3}}{t_{\bar{6}}E_3} - \frac{\delta\Delta_{\bar{6}63}}{t_6E_3}\right) - n_6^{-3}(n_6-1)d_{36}$	(T.3)	6%
#2	$r_{43} = -\sqrt{2}n_4^{-3}\left(\frac{\delta\Delta_{4\bar{4}4}}{t_{\bar{4}}E_4} + \frac{\delta\Delta_{\bar{4}4\bar{4}}}{t_4E_{\bar{4}}}\right) + n_4^{-3}(n_4-1)(d_{22}+d_{23}-d_{34}) - (r_{22}+r_{32})/2$	(T.4)	10%
	$r_{42} = -\sqrt{2}n_4^{-3}\left(\frac{\delta\Delta_{4\bar{4}4}}{t_{\bar{4}}E_4} - \frac{\delta\Delta_{\bar{4}4\bar{4}}}{t_4E_{\bar{4}}}\right) + n_4^{-3}(n_4-1)(d_{32}+d_{33}-d_{24}) - (r_{23}+r_{33})/2$	(T.5)	10%
#3	$r_{51} = -\sqrt{2}n_5^{-3}\left(\frac{\delta\Delta_{5\bar{5}5}}{t_{\bar{5}}E_5} - \frac{\delta\Delta_{\bar{5}5\bar{5}}}{t_5E_{\bar{5}}}\right) + n_5^{-3}(n_5-1)(d_{31}+d_{33}-d_{15}) - (r_{13}+r_{33})/2$	(T.6)	10%